Chen *et al. Satellite Navigation* (2024) 5:30
https://doi.org/10.1186/s43020-024-00151-8

ORIGINAL ARTICLE

Open Access

method is the basis for LiDAR Odometry (LO). Zhang and Singh (2014) developed a LiDAR Odometry and

road segment frame (*r*-frame) is defined. e origin is the optical center of the LiDAR sensor, and the three axes point towards the lateral, longitudinal, and up directions corresponding to the road surface, respectively.

SE-GPR based LO error model

Gaussian Process Regression (GPR) is a popular interpretable Bayesian model which demonstrates high predictive accuracy across various scenarios (Liu et al., 2020; Schulz et al., 2018). In this section, the proposed SE-GPR based LO error model is designed. Specifically, the LO error model is used to predict the error of LO-based vehicle displacement between two adjacent frames of point clouds to avoid the e ect of previous state estimation of LO. Originally, the LO-based displacement of the vehicle is calculated in the *l*-frame. With the estimated attitude, the displacement can be transformed to the one in the *n*-frame. In theory, the vehicle velocity determines the rel-

where V_{NPL}, V_{EPL}, and V_{HPL}

where $\delta \boldsymbol{r}_{e,\mathrm{IMU}}$, $\delta \boldsymbol{v}_{e,\mathrm{IMU}}$, and $\delta \boldsymbol{\varphi}_{e,\mathrm{IMU}}$ are the error vectors of IMU mechanization based position, velocity, and atti

multiple frequency GNSS receiver module was used to collect raw GNSS data at 10 Hz. And a Velodyne VLP-16 LiDAR sensor was used to collect raw point cloud data. e reference trajectories were determined by the RTK/INS tightly coupled post processing mode of NovAtel Inertial Explorer software with the raw data of a high-grade GNSS/IMU integrated navigator, Honeywell HGuide N580, with gyroscope bias instability of 0.25 (°)/h. In addition, the antenna 1 and 2 were connected with the BDStar Navigation receiver and the N580, respectively.

results of SE-GPR and other regression models over the training dataset are compared in Table 1. e candidate fitting models include coarse tree, fine Gaussian Support Vector Machine (SVM), and ensemble boosted regression tree. It is clear that the Root Mean Square Error (RMSE) of SE-GPR is the smallest among these candidate fitting models. R-squared is another important evaluation parameter with a value range between 0 and 1, and higher value indicates better fitting performance. It can be seen that the SE-GPR model provides the highest R-squared in fitting north, east, and down LO errors.

e testing dataset was collected in the downtown area of Nanjing city, about 8 km away from the location of the collected training dataset, on April 29, 2024. e vehicle trajectory of the testing dataset is shown in Fig. 5.

e vehicle was driven between dense and tall buildings for the whole trajectory. In several sections of the tra-

Table 2 Description of the tested algorithms

Candidate algorithm	Description
Basic GNSS/IMU/LO integration	GNSS/IMU/LO are loosely integrated with an EKF. The measurement vector is constructed with GNSS based position, doppler shifts based velocity and LO based position of the vehicle
Weighted GNSS/IMU/LO integration	GNSS/IMU/LO are integrated in a loosely coupled mode with an EKF. The measurement vector is constructed with the GNSS/LO weighting strategy based position and doppler shifts based velocity of the vehicle
Weighted GNSS/IMU/LO integration with LALC	GNSS/IMU/LO are integrated in a loosely coupled mode with an EKF. The measurement vector is constructed with the proposed GNSS/LO weighting strategy based position and doppler shifts based velocity of the vehicle. Besides, the proposed LALC is implemented
Weighted GNSS/IMU/LO integration with NHC	GNSS/IMU/LO are integrated in a loosely coupled mode with an EKF. The measurement vector is constructed with the proposed GNSS/LO weighting strategy based position and doppler shifts based velocity of the vehicle. Besides, the NHC is implemented
Proposed algorithm (Weighted GNSS/IMU/LO integration with the LALC and NHC)	GNSS/IMU/LO are integrated in a loosely coupled mode with an EKF. The measurement vector is constructed with the proposed GNSS/LO weighting strategy based position and doppler shifts based velocity of the vehicle. Besides, the proposed LALC and NHC are implemented

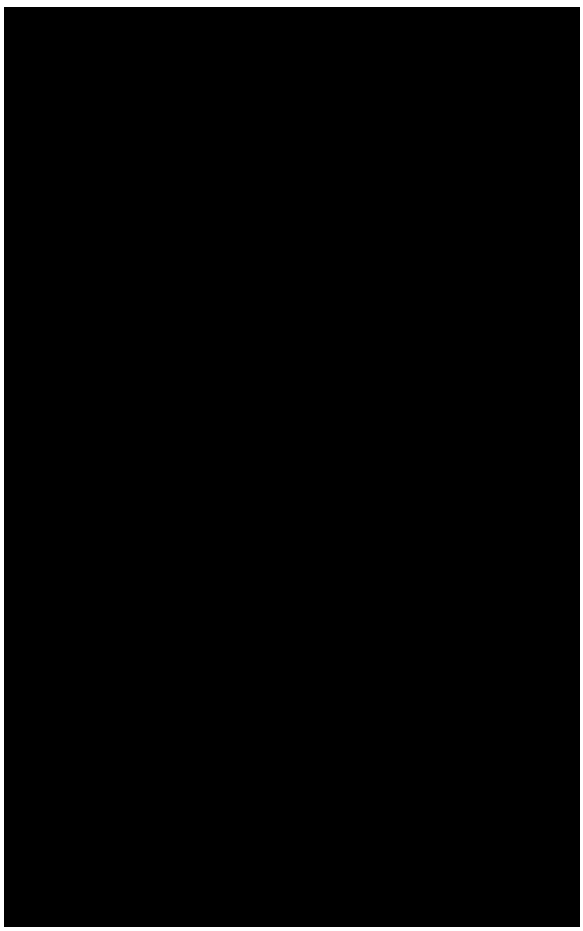

Fig. 11 Positioning error comparison in the *n*-frame. Figure shows positioning errors of the candidate algorithms in the *n*-frame, with green lines representing the "basic GNSS/IMU/LO integration" algorithm, purplish red lines representing the "weighted GNSS/IMU/

positioning erþÿ h4ss516red GNSS/IMU/

period from 410 to 440 s. Generally, the weighting coefficients vary correctly with the di erence of GNSS positioning and LO errors.

To validate the performance improvement of the proposed GNSS/IMU/LO integrated navigation algorithm, four candidate algorithms were also evaluated with the testing dataset. ese algorithms are described in Table 2.

Figure 11 compares the positioning errors of these algorithms in the *n*-frame. Figure 12 shows their horizontal positioning results in a real map. It is clear that the accuracy of horizontal positioning is improved significantly with the weighted GNSS/IMU/LO integration, especially from 80 to 130 s and from 240 to 310 s. By comparing the "weighted GNSS/IMU/LO integration" and the "weighted GNSS/IMU/LO integration with LALC", it is clear that the LALC improves horizontal